

Resonant Assisted Annihilation

Tarak Nath Maity,^a Tirtha Sankar Ray^{a,b}

^a*Department of Physics, Indian Institute of Technology Kharagpur, Kharagpur 721302, India*

^b*Centre for Theoretical Studies, Indian Institute of Technology Kharagpur, Kharagpur 721302, India*

E-mail: tarak.maity.physics@gmail.com, tirthasankar.ray@gmail.com

ABSTRACT: Assisted annihilation is a novel mechanism to generate viable sub-GeV thermal dark matter, where a pair of stable dark matter annihilates with an assister to Standard Model states. Typically such $3 \rightarrow 2$ annihilation topologies are flux suppressed compared to $2 \rightarrow 2$ processes. In this paper, we explore the possibility of a resonant $3 \rightarrow 2$ assisted annihilation dominantly driving the freeze-out of dark matter. We demonstrate that in a simple multipartite scalar extension of the Standard Model this can be realized in certain regions of parameter space to provide viable dark matter relic density in agreement with observation. We demonstrate that for photophilic assisters parts of parameter space are already constrained by indirect detection experiments while substantial regions remain beyond the present limit.

Contents

1	Introduction	1
2	Minimal Model for Resonant <i>Assisted Annihilation</i>	2
3	Relic Density	3
4	Phenomenology	5
4.1	Cosmological Constraint	6
4.2	Fixed Target Searches	6
4.3	Indirect Detection	6
5	Conclusions	9

1 Introduction

Sub-GeV dark matter (DM) scenarios have received recent attention from various quarters spurred by cosmological observation at the galactic scale in the context of structure formation [1–3]. Independently a lot of effort have been made to update the direct detection experiments to target sub-GeV weakly interacting DM [4–13]. These have led to a renewed interest in motivated model building for sub-GeV DM beyond the standard model [14]. Generically the direct detection experiment constraints scenarios that rely on the usual $2 \rightarrow 2$ annihilation topology providing a direct correlation between annihilation rates that set the relic density with direct detection cross sections. Generalization to more complicated topologies viz. $3 \rightarrow 2$, will keep these models insulated from the present and proposed direct detection experiments while a flux suppression in the DM annihilation process lead to lighter DM, landing in the cosmologically interesting sub-GeV mass range [15–34]. An effort in this direction is the so called *assisted annihilation* that was introduced in [19]. Minimal version of this class of models have a sub-GeV stable thermal DM state along with assisters that can promptly decay to SM. By construction the annihilation to SM states in the early universe is dominated by a $N \rightarrow 2$ topology where a pair of DM particles annihilate with one or more assisters in the initial state. This leads naturally to a thermal sub-GeV scale cold DM. Interestingly since the assisters are not charged under the same stabilizing symmetry as the DM it can in principle be lighter leading to a Boltzmann boost to the annihilation process [35]. There are non-trivial effect of these new light states on the cosmology of the early Universe. Some of the relevant constraints on this framework from Big Bang Nucleosynthesis (BBN) and Cosmic Microwave Background (CMB) have been explored in [35].

From the point of view of model building the challenge is to have the flux suppressed $3 \rightarrow 2$ channel dominate over possible $2 \rightarrow 2$ processes. A possibility of eliminating the

the $2 \rightarrow 2$ channel by a combination of kinematic phase space and Boltzmann suppression was presented in [35]. This required augmentation of the minimal setup to include a heavy mediator in addition to the DM and assister states. The object was to suppress the associated $2 \rightarrow 2$ process without tuning couplings. Keeping within this setup, in this paper we take the complimentary view of boosting the assisted annihilation process by tuning it near a resonance peak. For universal couplings the resonant s -channel mediated $3 \rightarrow 2$ can easily dominate over $2 \rightarrow 3$ and $2 \rightarrow 2$ processes. We find that for such scenarios it is easy to have an assisted annihilation dominated freeze-out of DM that saturates the observed relic abundance limits with perturbative couplings.

In this paper we present a simple scalar model of assisted annihilation containing a scalar \mathbb{Z}_2 odd DM, a photophilic scalar assister and a scalar mediator. We explore the region of parameter space where the assisted annihilation is near resonance. We demonstrate that within this framework it is easy to match the observed relic density of DM with perturbative couplings. We briefly comment on the possibility of probing a part of the allowed parameter space of this framework using indirect detection and beam dump experiments.

The paper is organized as follows. In section 2 we present the details of the minimal scalar model for resonant assisted annihilation. We make a systematic study of relic density of DM within this framework in section 3. We discuss the possibility of exploring this framework in indirect detection and beam dump experiments in section 4 before concluding.

2 Minimal Model for Resonant *Assisted Annihilation*

The minimal real scalar model for resonant assisted annihilation contains three real scalar fields viz. a stable DM (ϕ), a assister (A) and heavy mediator (S) which are all singlet under the SM gauge symmetries. The stability of the DM is ensured by assigning an odd charge to it under a discrete \mathbb{Z}_2 symmetry, while both the assisters and mediator can promptly decay to SM states which are all even under the same \mathbb{Z}_2 . The assister and the mediator also doubles up as a portal to the visible sector keeping DM in thermal equilibrium before freeze-out. The most general scalar potential for the dark sector and a photophilic portal coupling to the visible sector consistent with aforementioned charge assignments can be written as

$$\begin{aligned}
\mathcal{L}_{\text{dark}} = & \frac{1}{2}m_\phi^2\phi^2 + \frac{1}{2}m_A^2A^2 + \frac{1}{2}m_S^2S^2 \\
& + \frac{\lambda_1}{4}\phi^2A^2 + \frac{\lambda_2}{4}\phi^2S^2 + \frac{\lambda_3}{2}\phi^2AS + \frac{\lambda_4}{4}A^2S^2 \\
& + \frac{\lambda_5}{6}A^3S + \frac{\lambda_6}{6}S^3A + \mu_1\phi^2A + \mu_2\phi^2S \\
& + \frac{\mu_3}{6}A^3 + \frac{\mu_4}{6}S^3 + \frac{\mu_5}{2}A^2S + \frac{\mu_6}{2}S^2A \\
\mathcal{L}_{\text{portal}} = & c_\gamma^a AF^{\mu\nu}F_{\mu\nu} + c_\gamma^s SF^{\mu\nu}F_{\mu\nu},
\end{aligned} \tag{2.1}$$

where $F^{\mu\nu}$ is the standard electromagnetic field strength tensor and c_γ^a, c_γ^s have mass dimension of minus one. The non-renormalizable portal coupling of the dark sector to the SM represents a special choice which enables us to extract the most interesting phenomenological implications of the framework. Generalizations are straightforward and do not affect

the resonant assisted annihilation driven freeze-out of DM discussed in the next section. To keep the discussion tractable we will further assume all the λ_i , μ_i and c_γ^i of equation 2.1 to be universal and equal to λ , μ and c_γ respectively. We call this the Benchmark Model. As can be easily read out from the interactions given in equation 2.1 one of the

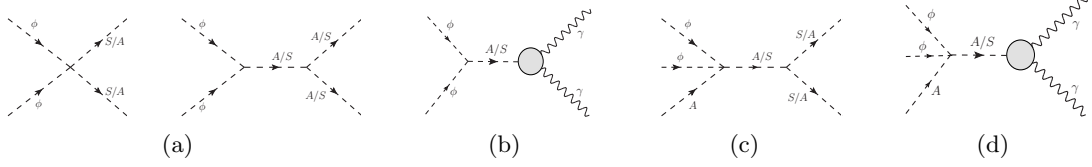


Figure 1: Feynman diagram of the relevant $2 \rightarrow 2$ and $3 \rightarrow 2$ processes.

annihilation channel for the DM proceed through the novel $3 \rightarrow 2$ topology given by $\phi\phi A \rightarrow S \rightarrow AA/\gamma\gamma$. Ordinarily this will be overwhelmed by a host of $2 \rightarrow 2$ processes like $\phi\phi \rightarrow SS/AA/AS$ etc. However in certain regions of the parameter space where the masses are tuned to put the assisted annihilation process on s -channel resonance this will dominantly drive out freeze-out of DM. In the next section we will explore this possibility of resonant assisted annihilation setting the DM relic density. Subsequently we will explore the phenomenological consequences of this framework.

3 Relic Density

In this section we will focus on the region of parameter space where a resonant assisted annihilation processes (shown in figure 1c and 1d) set the required relic density of DM [36]. Admittedly, this requires a tuning of masses of the dark sector states of the form, $(2m_\phi + m_A) \sim m_S$. The relevant Boltzmann equation is given by,

$$\frac{dY_\phi}{dx} = -\frac{s^2 g_*}{xH} N_{\text{Bolt}} \langle \sigma v^2 \rangle_{3 \rightarrow 2} \left[Y_\phi^2 Y_\phi^{\text{eq}} - \left(Y_\phi^{\text{eq}} \right)^3 \right] - \frac{s g_*}{xH} \langle \sigma v \rangle_{2 \rightarrow 2} \left[Y_\phi^2 - \left(Y_\phi^{\text{eq}} \right)^2 \right] \quad (3.1a)$$

$$N_{\text{Bolt}} = e^{qx(1-\epsilon)} \epsilon^{3/2}, \quad g_* = 1 + \frac{1}{3} \frac{d(\ln g_s)}{d(\ln T)}, \quad (3.1b)$$

where $x = m_\phi/T$, $\epsilon = m_A/m_\phi$, entropy density $s = 2\pi^2 g_s T^3/45$, Hubble constant $H = \sqrt{\pi^2 g_\rho/90} (T^2/M_{\text{Pl}})$, g_s and g_ρ are the effective number of relativistic degrees of freedom corresponding to entropy and energy density respectively. For the temperature dependence of g_ρ , g_s and g_* we have followed [37]. The thermally averaged cross section $\langle \sigma v^2 \rangle_{3 \rightarrow 2}$ includes all $3 \rightarrow 2$ processes while $\langle \sigma v \rangle_{2 \rightarrow 2}$ quantify the sub-dominant $2 \rightarrow 2$ annihilation cross sections¹. Note that, for $\epsilon > 1$ there will be a Boltzmann suppression of the initial state assister flux while for $\epsilon < 1$ there is a enhancement of the effective cross section for similar reasons. This is a novel feature of the assisted annihilation framework that should

¹In principle to obtain the correct relic density full set of coupled Boltzmann equations involving the DM, assisters and mediator should be considered. However, at resonance, equation (3.1) reproduces the results adequately.

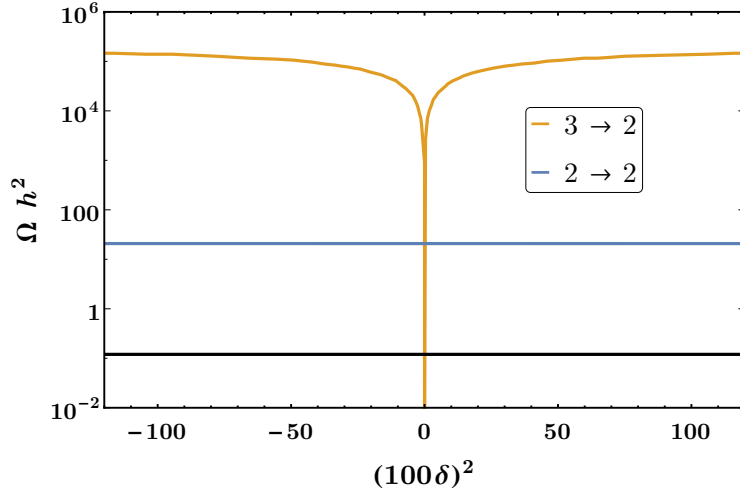


Figure 2: Relic density as a function of $(100\delta)^2$, where δ has been defined in equation (3.2). The light blue and light orange line shows Ωh^2 estimated using $2 \rightarrow 2$ and $3 \rightarrow 2$ channels. We set $m_\phi = 200$ MeV, $m_A = 100$ MeV, $\lambda = 10^{-5}$, $\mu/m_\phi = 10^{-3}$ and $c_\gamma = 10^{-11}$ MeV $^{-1}$.

be contrasted with the usual co-annihilation scenario, where by construction a Boltzmann suppression is obtained depending on the mass-splitting of the co-annihilating states [35]. The relevant Feynman diagrams of $2 \rightarrow 2$ processes are shown in figure 1a and 1b while the Feynman diagrams of $3 \rightarrow 2$ assisted annihilation processes are shown in figure 1c and 1d. Note that the cross section of both $3 \rightarrow 2$ and $2 \rightarrow 2$ processes depend on λ , μ and c_γ . In spite of the strong constraint on c_γ from fixed target experiments [38] with λ and $\mu/m_\phi \sim \mathcal{O}(1)$ the $2 \rightarrow 2$ processes in general will dominate. However, in the region of parameter space where the masses are tuned so that $(2m_\phi + m_A) \sim m_S$, the $3 \rightarrow 2$ assisted annihilation, now set at resonance, can dominantly drive freeze-out to saturate the required relic density bound. To illustrate the effect of resonance on relic density we define following parameter

$$\delta^2 \equiv \frac{(2m_\phi + m_A)^2 - m_S^2}{m_\phi^2} \quad (3.2)$$

The relevant thermally averaged $3 \rightarrow 2$ cross section is inversely proportional to $\delta^4 m_\phi^4 + \Gamma_S^2 m_S^2$, where Γ_S is the decay width of S , which sets the peak value of the cross section at resonance. In figure 2 relic density is plotted as a function of $(100\delta)^2$, keeping $m_\phi = 200$ MeV, $\epsilon = 0.5$, $\lambda = 10^{-5}$, $\mu/m_\phi = 10^{-3}$, $c_\gamma = 10^{-11}$ MeV $^{-1}$. The sharp fall in the orange line around $\delta = 0$ signify the resonance effect. The relic density keeping only the corresponding $2 \rightarrow 2$ processes in equation (3.1) is shown by the light blue line. The black solid band shows allowed range of DM relic density ($\Omega h^2 = 0.12 \pm 0.0001$) [36]. Clearly, a resonant $3 \rightarrow 2$ assisted annihilation can effectively drive freeze-out to obtain the required relic density.

As is evident from the definition in equation (3.2), δ determines how close a parameter

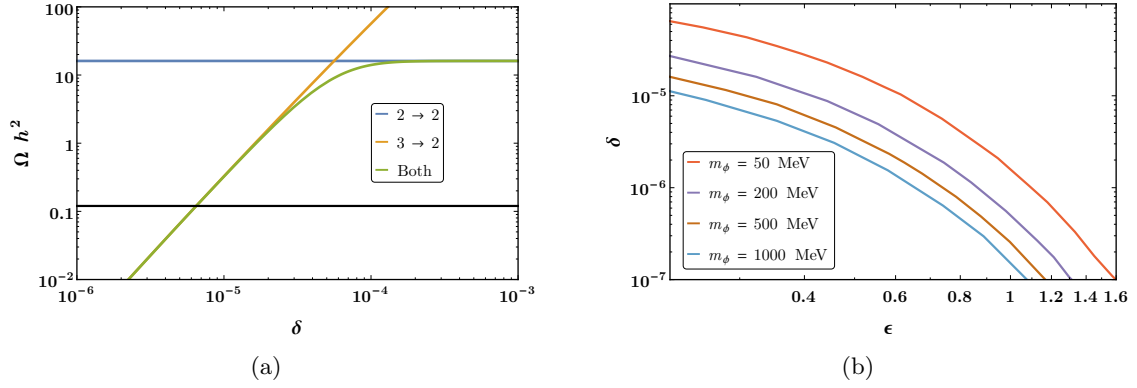


Figure 3: (a) Comparison of relic density evaluated using $2 \rightarrow 2$ processes (light blue), $3 \rightarrow 2$ processes (light orange) and combining both of them (light green) in $\delta - \Omega h^2$ plane. The horizontal black solid line denotes the allowed relic density. (b) Relic density allowed contours in ϵ vs δ plane. The light red, light violet, light brown and sky blue lines corresponds to $m_\phi = 50$ MeV, $m_\phi = 200$ MeV, $m_\phi = 500$ MeV and $m_\phi = 1000$ MeV respectively. For both the panels other couplings are: $\lambda = 10^{-5}$, $\mu/m_\phi = 10^{-5}$, $c_\gamma = 10^{-11}$ MeV $^{-1}$.

point is to resonance and therefore is a measure of tuning in the theory. As δ decreases the $3 \rightarrow 2$ assisted annihilation contribution to the relic density starts dominating and the contribution of the $2 \rightarrow 2$ increasingly become numerically insignificant. This can be seen from figure 3a, which suggests that the $\phi\phi A \rightarrow S \rightarrow AA$ and $\phi\phi A \rightarrow \gamma\gamma$ channels become predominant below $\delta \leq 10^{-4}$. In figure 3b, DM relic density allowed contours for DM masses $m_\phi = 50, 200, 500$ and 1000 MeV has been displayed in $\epsilon - \delta$ plane. For $\epsilon < 1$ the effect of Boltzmann boost [35] helps to achieve the required relic abundance with relatively larger value of δ while for $\epsilon > 1$ due to the Boltzmann suppression resonance effect has to be more pronounced to satisfy the relic density constraint.

4 Phenomenology

Being immune to direct detection experiments the $3 \rightarrow 2$ assisted annihilation framework is amenable to probing through indirect effects. First we examine the cosmological implications of the light states, especially the late decay of the photophilic MeV scale assisters. Beam dump experiments can put complimentary constraints on the photophilic assisters. Finally the γ -ray flux arising from associated DM annihilation at present day universe may be of interest in the context of indirect detection experiments. We now elaborate on these phenomenological consequences of the resonant assisted annihilation framework in the context of the model presented in section 2.

4.1 Cosmological Constraint

Any coupling between the MeV scale assister/mediator (A/S) to the photon will have several cosmological implications. A detailed discussion on this can be found in [35]. The late time decay of the A/S to photons may lead to photo-dissociation of the BBN products [39–45]. This essentially puts an upper bound on the lifetime of the decaying species. Here we use a conservative limit on lifetime of both the assister and the mediator, to be less than 1 s, and fix c_γ to $10^{-11} \text{ MeV}^{-1}$ which is also consistent with beam dump experiments discussed next. Additionally, light degrees of freedom can increase Hubble expansion rate which may alter BBN yields, constraining the masses to be greater than 1 MeV [46]. Other than these, the direct annihilation to photons after neutrino decoupling may change photon to neutrino temperature ratio [47–51]. However, in the resonant assisted annihilation framework the direct annihilation to photons stalls well before neutrino decoupling in the parameter space of interest owing primarily due to the smallness of c_γ .

4.2 Fixed Target Searches

An alternate strategy to search for photophilic A/S is through fixed target experiments. There are several experiments like PRIMEX [38], GLUEX [38], E137 [52], Belle-II [53], SHiP [54], FASER2 [55], SeaQuest [56], and NA 62 [57] which may probe the effective photon coupling c_γ of A/S . A conservative limit of $c_\gamma \leq 10^{-11} \text{ MeV}^{-1}$ is found to be in consonance with the exclusion bounds in the mass range of interest [35].

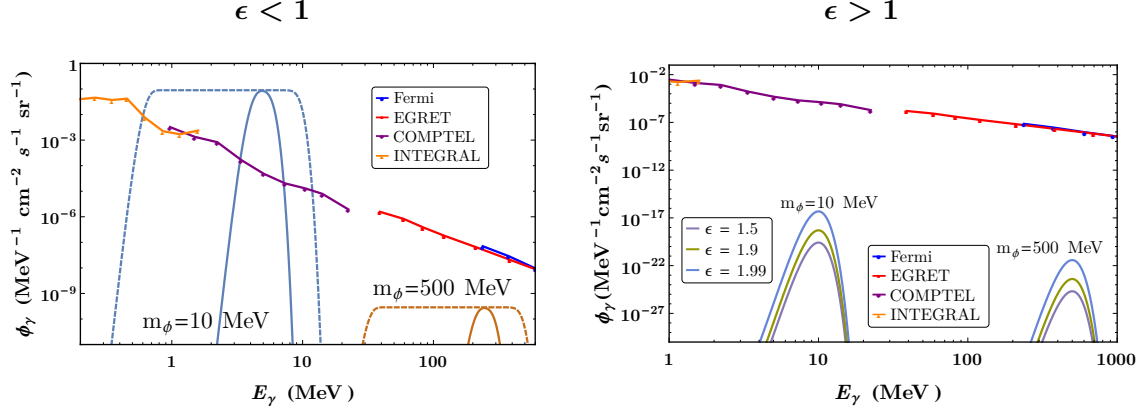
4.3 Indirect Detection

In our region of interest the dominant contribution to the relic density is driven by the s -channel resonant assisted annihilation processes, shown in figure 1c and 1d. However, this $3 \rightarrow 2$ annihilation processes is inoperative once the assister number density plummets due to decay. Interestingly, the $2 \rightarrow 2$ sub-dominant processes given in figure 1a and 1b survives and provides a handle to explore these framework through indirect detection. In the most generic form of the Lagrangian in equation (2.1) it is possible to tune the couplings to drive resonant assisted annihilation while keeping all the relevant cross sections negligible. However, in the benchmark model a sizable resonant assisted annihilation would lead to correlated cross section of indirect detection. It is in this context we explore the possibility to probe parameter space of the benchmark model through indirect detection.

For the presented model, photophilic assister may produce potential γ -ray flux. The differential photon flux from the annihilation of a self-conjugate DM is given by [58]

$$\Phi'_\gamma(E_\gamma) = \frac{\rho_\odot^2 r_\odot}{8\pi m_\phi^2} \sum_i \langle \sigma v \rangle_i \frac{dN_\gamma^i}{dE_\gamma} \frac{J}{\Delta\Omega}, \quad (4.1)$$

where $\langle \sigma v \rangle_i$ is the thermally averaged annihilation cross section, dN_γ^i/dE_γ is the corresponding spectrum of γ -rays, $r_\odot \simeq 8.5 \text{ kpc}$ is the Sun's distance from the Galactic center, $\rho_\odot \simeq 0.3 \text{ GeV/cm}^3$ is the local DM density, and J is the standard J -factor which integrates intermediate DM density along the line of sight over the solid angle $\Delta\Omega$. We have used NFW profile [59, 60] to calculate J factor for the experiments [61]. The dominant contribution on the γ -ray flux comes from two different kinds of processes



(a) Convoluted gamma-ray flux $\Phi_\gamma(E_\gamma)$ for two DM masses of 10 MeV and 500 MeV by light blue and light green lines respectively. The value of λ has been set to 10^{-5} . The solid lines represent $\epsilon = 0.99$ while dashed lines are for $\epsilon = 0.5$.

(b) Smeared gamma-ray flux $\Phi_\gamma(E_\gamma)$ for two DM masses of 10 MeV and 500 MeV with $\epsilon > 1$. Three different colors are for three choices of ϵ as displayed in the legend.

Figure 4: The chosen values of remaining parameters mentioned in figure 3.

1. Two body annihilation to assisters as shown in figure 1a. In the center-of-mass frame of the DM, the subsequent decay of the assisters to photons will develop a box-shaped spectra for the former. The spectra of the photon can be written as [62, 63]

$$\frac{dN_\gamma}{dE_\gamma} = \frac{4}{\Delta E} \Theta(E_\gamma - E_-) \Theta(E_\gamma - E_+), \quad (4.2)$$

where

$$E_\pm = \frac{m_\phi}{2} \left(1 \pm \sqrt{1 - \frac{m_A^2}{m_\phi^2}} \right)$$

are the edges of the box and ΔE is the difference between them and Θ is the step function. This channel will be operative only for $\epsilon < 1$.

2. Direct two body annihilation to photons as depicted in figure 1b, which will be functional both for $\epsilon < 1$ and $\epsilon > 1$. In the center-of-mass frame of the DM this would give rise to following line spectra of the photons

$$\frac{dN_\gamma}{dE_\gamma} = 2 \delta(E_\gamma - m_\phi), \quad (4.3)$$

where $\delta(E_\gamma - m_\phi)$ is the Dirac delta function, not to be confused with δ defined in equation (3.2). We have assumed a Gaussian detector response [64] which would spread out the spikes and sharp kinematic edges of the flux ($\Phi'_\gamma(E_\gamma)$) and the convoluted gamma-ray flux ($\Phi_\gamma(E_\gamma)$) has been compared with the experimental results. There have been several gamma-ray satellites which search for such flux from DM annihilation. Since we are exploring phenomenology of DM mass in sub-GeV range, therefore we have used outcome

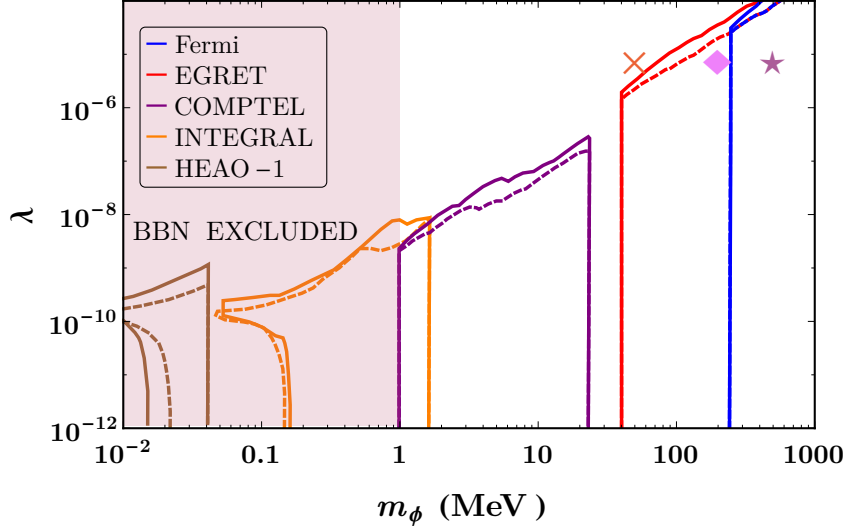


Figure 5: Allowed regions of λ as a function of DM mass m_ϕ . The upper limit on λ from HEAO-1, INTEGRAL, COMPTEL, EGRET and Fermi is shown by brown, orange, purple, red, and blue lines respectively. The BBN excluded region is shown by light red shading. The solid and dashed lines of each colour correspond to $\epsilon = 0.99$ and $\epsilon = 0.5$ respectively. The other parameters are same as in figure 3.

of low energy gamma-ray detector like HEAO-1 [65], INTEGRAL [66], COMPTEL [67, 68], EGRET [69] and Fermi [70] to obtain the constraint on the relevant parameters of the model presented in section 2. We have used central values of the observations of the experiments and interpolated that to obtain a continuous flux in their respective energy window.

In figures 4a and 4b we have shown smeared differential gamma-ray flux ($\Phi_\gamma(E_\gamma)$) as a function of gamma-ray energy for $\epsilon < 1$ and $\epsilon > 1$ respectively. For $\epsilon < 1$ both $\phi\phi \rightarrow 4\gamma$ through A and $\phi\phi \rightarrow \gamma\gamma$ is operative. However, from BBN and fixed target constraints on c_γ and for $\mu/m_\phi = 10^{-5}$ contribution of former to the total flux is numerically insignificant, this leads to box type spectrum as shown in figure 4a. Apart from this, with the choice $\lambda = \mu/m_\phi = 10^{-5}$, DM annihilation to assisters through point interaction would dominate the same annihilation through A/S mediation. For $\epsilon > 1$ only channel to probe DM signals through indirect detection is $\phi\phi \rightarrow \gamma\gamma$. However, in the region of parameter space where resonance assisted annihilation is the dominant channel to drive the freeze-out, smallness of μ and c_γ makes the differential gamma-ray flux beyond the reach of the current experimental sensitivity. This has been shown in figure 4b for DM masses 10 and 500 MeV. Since the thermally averaged cross section $\langle\sigma v\rangle_i$ of a particular channel is inversely proportional to m_ϕ^2 , therefore for a fixed choice of other couplings and masses the maximum value of flux increases with decrease in DM mass.

The upper limit on λ for the benchmark model from HEAO-1, INTEGRAL, COMPTEL, EGRET and Fermi against the DM mass is shown in figure 5. For completeness, three benchmark points which satisfy the relic density constraint are shown by star, diamond

Table 1: Benchmark points

BP	m_ϕ (MeV)	λ	c_γ MeV^{-1}	μ/m_ϕ	ϵ	δ	Flux $\Phi_\gamma(E_+)$ $(\text{MeV s sr})^{-1} \text{ cm}^{-2}$
BP1 \times	50	10^{-5}	10^{-11}	10^{-5}	0.99	1.67×10^{-6}	1.3×10^{-5}
					0.5	1.8×10^{-5}	1.3×10^{-5}
BP2 \diamond	200	10^{-5}	10^{-11}	10^{-5}	0.99	5.3×10^{-7}	1.3×10^{-8}
					0.5	5.3×10^{-6}	1.3×10^{-8}
BP3 \star	500	10^{-5}	10^{-11}	10^{-5}	0.99	2.7×10^{-6}	1.3×10^{-10}
					0.5	3.7×10^{-6}	1.3×10^{-10}

and cross. The details of the benchmark points are given in table 1.

5 Conclusions

In this paper we present an alternate possibility to drive thermal freeze-out, through a multi-body $3 \rightarrow 2$ resonant assisted annihilation. Here along with a pair of DM there is an SM-like assister in the initial state. The key challenge here is to overcome the contribution of related $2 \rightarrow 2$ channels in comparison to these flux suppressed multi-body $3 \rightarrow 2$ assisted annihilation processes. In this paper we have presented a simple model having a three real scalars, a stable DM (ϕ), an assister (A) and a heavy mediator (S) where the latter two also double up as a portal to the visible sector. We find that in the region of parameter space where masses are tuned to $(2m_\phi + m_A) \sim m_S$ an s -channel $3 \rightarrow 2$ assisted annihilation channel can have resonance and dominantly drive freeze-out to produce the observed relic density of DM. We show that in this tuned region the relic abundance is in the right ballpark for a DM mass between 100 MeV to a few GeV with perturbative couplings.

The resonant assisted annihilation channels are difficult to probe in direct detection experiments owing to its novel topology. In this article we have showed that even in the distinctive resonance region, the correlated $2 \rightarrow 2$ annihilation channels can produce appreciable indirect detection signatures. Annihilation of the DM to assisters and subsequent decay of the photophilic assister can be constrained by excrements like HEAO-1, INTEGRAL, EGERET, COMPTEL, Fermi in certain regions of the parameter space.

Acknowledgments: We would like to thank Ujjal Kumar Dey for comments on the manuscript. TNM would like to thank MHRD, Government of India for a research fellowship. TSR is partially supported by the Department of Science and Technology, Government of India, under the Grant Agreement No. IFA13-PH-74 (INSPIRE Faculty Award).

References

- [1] D. N. Spergel and P. J. Steinhardt, *Observational evidence for selfinteracting cold dark matter*, *Phys. Rev. Lett.* **84** (2000) 3760–3763, [[astro-ph/9909386](#)].
- [2] T. Nakama, J. Chluba and M. Kamionkowski, *Shedding light on the small-scale crisis with CMB spectral distortions*, *Phys. Rev.* **D95** (2017) 121302, [[1703.10559](#)].

- [3] J. S. Bullock and M. Boylan-Kolchin, *Small-Scale Challenges to the Λ CDM Paradigm*, *Ann. Rev. Astron. Astrophys.* **55** (2017) 343–387, [[1707.04256](#)].
- [4] SENSEI collaboration, M. Crisler, R. Essig, J. Estrada, G. Fernandez, J. Tiffenberg, M. Sofo haro et al., *SENSEI: First Direct-Detection Constraints on sub-GeV Dark Matter from a Surface Run*, *Phys. Rev. Lett.* **121** (2018) 061803, [[1804.00088](#)].
- [5] SENSEI collaboration, O. Abramoff et al., *SENSEI: Direct-Detection Constraints on Sub-GeV Dark Matter from a Shallow Underground Run Using a Prototype Skipper-CCD*, *Phys. Rev. Lett.* **122** (2019) 161801, [[1901.10478](#)].
- [6] R. Essig, J. Mardon and T. Volansky, *Direct Detection of Sub-GeV Dark Matter*, *Phys. Rev.* **D85** (2012) 076007, [[1108.5383](#)].
- [7] R. Essig, M. Fernandez-Serra, J. Mardon, A. Soto, T. Volansky and T.-T. Yu, *Direct Detection of sub-GeV Dark Matter with Semiconductor Targets*, *JHEP* **05** (2016) 046, [[1509.01598](#)].
- [8] S. K. Lee, M. Lisanti, S. Mishra-Sharma and B. R. Safdi, *Modulation Effects in Dark Matter-Electron Scattering Experiments*, *Phys. Rev.* **D92** (2015) 083517, [[1508.07361](#)].
- [9] Y. Hochberg, T. Lin and K. M. Zurek, *Absorption of light dark matter in semiconductors*, *Phys. Rev.* **D95** (2017) 023013, [[1608.01994](#)].
- [10] N. A. Kurinsky, T. C. Yu, Y. Hochberg and B. Cabrera, *Diamond Detectors for Direct Detection of Sub-GeV Dark Matter*, [[1901.07569](#)].
- [11] Y. Hochberg, Y. Zhao and K. M. Zurek, *Superconducting Detectors for Superlight Dark Matter*, *Phys. Rev. Lett.* **116** (2016) 011301, [[1504.07237](#)].
- [12] Y. Hochberg, T. Lin and K. M. Zurek, *Detecting Ultralight Bosonic Dark Matter via Absorption in Superconductors*, *Phys. Rev.* **D94** (2016) 015019, [[1604.06800](#)].
- [13] Y. Hochberg, I. Charaev, S.-W. Nam, V. Verma, M. Colangelo and K. K. Berggren, *Detecting Dark Matter with Superconducting Nanowires*, [[1903.05101](#)].
- [14] M. Battaglieri et al., *US Cosmic Visions: New Ideas in Dark Matter 2017: Community Report*, in *U.S. Cosmic Visions: New Ideas in Dark Matter College Park, MD, USA, March 23-25, 2017*, 2017. [[1707.04591](#)].
- [15] A. D. Dolgov, *ON CONCENTRATION OF RELICT THETA PARTICLES. (IN RUSSIAN)*, *Yad. Fiz.* **31** (1980) 1522–1528.
- [16] A. D. Dolgov, *New Old Mechanism of Dark Matter Burning*, [[1705.03689](#)].
- [17] Y. Hochberg, E. Kuflik, T. Volansky and J. G. Wacker, *Mechanism for Thermal Relic Dark Matter of Strongly Interacting Massive Particles*, *Phys. Rev. Lett.* **113** (2014) 171301, [[1402.5143](#)].
- [18] Y. Hochberg, E. Kuflik, H. Murayama, T. Volansky and J. G. Wacker, *Model for Thermal Relic Dark Matter of Strongly Interacting Massive Particles*, *Phys. Rev. Lett.* **115** (2015) 021301, [[1411.3727](#)].
- [19] U. K. Dey, T. N. Maity and T. S. Ray, *Light Dark Matter through Assisted Annihilation*, *JCAP* **1703** (2017) 045, [[1612.09074](#)].
- [20] N. Bernal and X. Chu, *\mathbb{Z}_2 SIMP Dark Matter*, *JCAP* **1601** (2016) 006, [[1510.08527](#)].
- [21] H. M. Lee and M.-S. Seo, *Models for SIMP dark matter and dark photon*, *AIP Conf. Proc.* **1743** (2016) 060003, [[1510.05116](#)].

- [22] S.-M. Choi and H. M. Lee, *SIMP dark matter with gauged Z_3 symmetry*, *JHEP* **09** (2015) 063, [[1505.00960](#)].
- [23] N. Bernal, C. Garcia-Cely and R. Rosenfeld, *WIMP and SIMP Dark Matter from the Spontaneous Breaking of a Global Group*, *JCAP* **1504** (2015) 012, [[1501.01973](#)].
- [24] Y. Hochberg, E. Kuflik and H. Murayama, *SIMP Spectroscopy*, *JHEP* **05** (2016) 090, [[1512.07917](#)].
- [25] E. Kuflik, M. Perelstein, N. R.-L. Lorier and Y.-D. Tsai, *Elastically Decoupling Dark Matter*, *Phys. Rev. Lett.* **116** (2016) 221302, [[1512.04545](#)].
- [26] S.-M. Choi, Y.-J. Kang and H. M. Lee, *On thermal production of self-interacting dark matter*, *JHEP* **12** (2016) 099, [[1610.04748](#)].
- [27] S.-M. Choi and H. M. Lee, *Resonant SIMP dark matter*, *Phys. Lett. B* **758** (2016) 47–53, [[1601.03566](#)].
- [28] N. Bernal, X. Chu and J. Pradler, *Simply split strongly interacting massive particles*, *Phys. Rev. D* **95** (2017) 115023, [[1702.04906](#)].
- [29] S.-Y. Ho, T. Toma and K. Tsumura, *A Radiative Neutrino Mass Model with SIMP Dark Matter*, *JHEP* **07** (2017) 101, [[1705.00592](#)].
- [30] J. M. Cline, H. Liu, T. Slatyer and W. Xue, *Enabling Forbidden Dark Matter*, *Phys. Rev. D* **96** (2017) 083521, [[1702.07716](#)].
- [31] S.-M. Choi, Y. Hochberg, E. Kuflik, H. M. Lee, Y. Mambrini, H. Murayama et al., *Vector SIMP dark matter*, *JHEP* **10** (2017) 162, [[1707.01434](#)].
- [32] E. Kuflik, M. Perelstein, N. R.-L. Lorier and Y.-D. Tsai, *Phenomenology of ELDER Dark Matter*, *JHEP* **08** (2017) 078, [[1706.05381](#)].
- [33] Y. Hochberg, E. Kuflik, R. McGehee, H. Murayama and K. Schutz, *Strongly interacting massive particles through the axion portal*, *Phys. Rev. D* **98** (2018) 115031, [[1806.10139](#)].
- [34] Y. Hochberg, E. Kuflik and H. Murayama, *Twin Higgs model with strongly interacting massive particle dark matter*, *Phys. Rev. D* **99** (2019) 015005, [[1805.09345](#)].
- [35] U. K. Dey, T. N. Maity and T. S. Ray, *Boosting Assisted Annihilation for a Cosmologically Safe MeV Scale Dark Matter*, *Phys. Rev. D* **99** (2019) 095025, [[1812.11418](#)].
- [36] PLANCK collaboration, N. Aghanim et al., *Planck 2018 results. VI. Cosmological parameters*, [1807.06209](#).
- [37] M. Drees, F. Hajkarim and E. R. Schmitz, *The Effects of QCD Equation of State on the Relic Density of WIMP Dark Matter*, *JCAP* **1506** (2015) 025, [[1503.03513](#)].
- [38] D. Aloni, C. Fanelli, Y. Soreq and M. Williams, *Photoproduction of axion-like particles*, [1903.03586](#).
- [39] R. J. Protheroe, T. Stanev and V. S. Berezinsky, *Electromagnetic cascades and cascade nucleosynthesis in the early universe*, *Phys. Rev. D* **51** (1995) 4134–4144, [[astro-ph/9409004](#)].
- [40] M. Kawasaki and T. Moroi, *Electromagnetic cascade in the early universe and its application to the big bang nucleosynthesis*, *Astrophys. J.* **452** (1995) 506, [[astro-ph/9412055](#)].
- [41] R. H. Cyburt, J. R. Ellis, B. D. Fields and K. A. Olive, *Updated nucleosynthesis constraints on unstable relic particles*, *Phys. Rev. D* **67** (2003) 103521, [[astro-ph/0211258](#)].

- [42] K. Jedamzik, *Big bang nucleosynthesis constraints on hadronically and electromagnetically decaying relic neutral particles*, *Phys. Rev.* **D74** (2006) 103509, [[hep-ph/0604251](#)].
- [43] V. Poulin and P. D. Serpico, *Nonuniversal BBN bounds on electromagnetically decaying particles*, *Phys. Rev.* **D91** (2015) 103007, [[1503.04852](#)].
- [44] M. Hufnagel, K. Schmidt-Hoberg and S. Wild, *BBN constraints on MeV-scale dark sectors. Part II. Electromagnetic decays*, *JCAP* **1811** (2018) 032, [[1808.09324](#)].
- [45] L. Forestell, D. E. Morrissey and G. White, *Limits from BBN on Light Electromagnetic Decays*, *JHEP* **01** (2019) 074, [[1809.01179](#)].
- [46] R. H. Cyburt, B. D. Fields, K. A. Olive and T.-H. Yeh, *Big Bang Nucleosynthesis: 2015*, *Rev. Mod. Phys.* **88** (2016) 015004, [[1505.01076](#)].
- [47] E. W. Kolb, M. S. Turner and T. P. Walker, *The Effect of Interacting Particles on Primordial Nucleosynthesis*, *Phys. Rev.* **D34** (1986) 2197.
- [48] P. D. Serpico and G. G. Raffelt, *MeV-mass dark matter and primordial nucleosynthesis*, *Phys. Rev.* **D70** (2004) 043526, [[astro-ph/0403417](#)].
- [49] K. M. Nollett and G. Steigman, *BBN And The CMB Constrain Light, Electromagnetically Coupled WIMPs*, *Phys. Rev.* **D89** (2014) 083508, [[1312.5725](#)].
- [50] K. M. Nollett and G. Steigman, *BBN And The CMB Constrain Neutrino Coupled Light WIMPs*, *Phys. Rev.* **D91** (2015) 083505, [[1411.6005](#)].
- [51] P. F. Depta, M. Hufnagel, K. Schmidt-Hoberg and S. Wild, *BBN constraints on the annihilation of MeV-scale dark matter*, *JCAP* **1904** (2019) 029, [[1901.06944](#)].
- [52] J. D. Bjorken, S. Ecklund, W. R. Nelson, A. Abashian, C. Church, B. Lu et al., *Search for Neutral Metastable Penetrating Particles Produced in the SLAC Beam Dump*, *Phys. Rev.* **D38** (1988) 3375.
- [53] M. J. Dolan, T. Ferber, C. Hearty, F. Kahlhoefer and K. Schmidt-Hoberg, *Revised constraints and Belle II sensitivity for visible and invisible axion-like particles*, *JHEP* **12** (2017) 094, [[1709.00009](#)].
- [54] S. Alekhin et al., *A facility to Search for Hidden Particles at the CERN SPS: the SHiP physics case*, *Rept. Prog. Phys.* **79** (2016) 124201, [[1504.04855](#)].
- [55] J. L. Feng, I. Galon, F. Kling and S. Trojanowski, *Axionlike particles at FASER: The LHC as a photon beam dump*, *Phys. Rev.* **D98** (2018) 055021, [[1806.02348](#)].
- [56] A. Berlin, S. Gori, P. Schuster and N. Toro, *Dark Sectors at the Fermilab SeaQuest Experiment*, *Phys. Rev.* **D98** (2018) 035011, [[1804.00661](#)].
- [57] B. Döbrich, J. Jaeckel, F. Kahlhoefer, A. Ringwald and K. Schmidt-Hoberg, *ALPtraum: ALP production in proton beam dump experiments*, *JHEP* **02** (2016) 018, [[1512.03069](#)].
- [58] T. R. Slatyer, *Indirect Detection of Dark Matter*, in *Proceedings, Theoretical Advanced Study Institute in Elementary Particle Physics : Anticipating the Next Discoveries in Particle Physics (TASI 2016): Boulder, CO, USA, June 6-July 1, 2016*, pp. 297–353, 2018. [[1710.05137](#)]. DOI.
- [59] J. F. Navarro, C. S. Frenk and S. D. M. White, *The Structure of cold dark matter halos*, *Astrophys. J.* **462** (1996) 563–575, [[astro-ph/9508025](#)].
- [60] J. F. Navarro, C. S. Frenk and S. D. M. White, *A Universal density profile from hierarchical clustering*, *Astrophys. J.* **490** (1997) 493–508, [[astro-ph/9611107](#)].

- [61] R. Essig, E. Kuflik, S. D. McDermott, T. Volansky and K. M. Zurek, *Constraining Light Dark Matter with Diffuse X-Ray and Gamma-Ray Observations*, *JHEP* **11** (2013) 193, [[1309.4091](#)].
- [62] A. Ibarra, S. Lopez Gehler and M. Pato, *Dark matter constraints from box-shaped gamma-ray features*, *JCAP* **1207** (2012) 043, [[1205.0007](#)].
- [63] K. K. Boddy and J. Kumar, *Indirect Detection of Dark Matter Using MeV-Range Gamma-Ray Telescopes*, *Phys. Rev.* **D92** (2015) 023533, [[1504.04024](#)].
- [64] T. Bringmann, M. Doro and M. Fornasa, *Dark Matter signals from Draco and Willman 1: Prospects for MAGIC II and CTA*, *JCAP* **0901** (2009) 016, [[0809.2269](#)].
- [65] D. E. Gruber, J. L. Matteson, L. E. Peterson and G. V. Jung, *The spectrum of diffuse cosmic hard x-rays measured with heao-1*, *Astrophys. J.* **520** (1999) 124, [[astro-ph/9903492](#)].
- [66] L. Bouchet, E. Jourdain, J. P. Roques, A. Strong, R. Diehl, F. Lebrun et al., *INTEGRAL SPI All-Sky View in Soft Gamma Rays: Study of Point Source and Galactic Diffuse Emissions*, *Astrophys. J.* **679** (2008) 1315, [[0801.2086](#)].
- [67] G. Weidenspointner, *The Origin of the Cosmic Gamma-Ray Background in the COMPTEL Energy Range*. PhD thesis, Technical University of Munich, Munich, Germany, 1999.
- [68] S. C. Kappadath, *Measurement of the Cosmic Diffuse Gamma-Ray Spectrum from 800 keV to 30 MeV*. PhD thesis, University of New Hampshire, 1998.
- [69] A. W. Strong, I. V. Moskalenko and O. Reimer, *Diffuse galactic continuum gamma rays. A Model compatible with EGRET data and cosmic-ray measurements*, *Astrophys. J.* **613** (2004) 962–976, [[astro-ph/0406254](#)].
- [70] FERMI-LAT collaboration, M. Ackermann et al., *Fermi-LAT Observations of the Diffuse Gamma-Ray Emission: Implications for Cosmic Rays and the Interstellar Medium*, *Astrophys. J.* **750** (2012) 3, [[1202.4039](#)].